OPEN ACCESS

Saudi Journal of Civil Engineering
Abbreviated Key Title: Saudi J Civ Eng
ISSN 2523-2657 (Print) |ISSN 2523-2231 (Online)
Scholars Middle East Publishers, Dubai, United Arab Emirates
Journal homepage: https://saudijournals.com/journal/sjce/home

Original Research Article

Microstructure Characteristic and Mechanical Properties of Copper Influenced Grey Cast Iron

Kutelu, B. J[1], Ogundeji, O. O[1*], Oluyori, R. T[1]

[1]Department of Mineral and Petroleum Engineering Technology, The Federal Polytechnic, Ado-Ekiti, Ekiti, State, Nigeria

DOI: 10.36348/sjce.2024.v08i05.001 | **Received:** 24.03.2024 | **Accepted:** 02.05.2024 | **Published:** 18.05.2024

***Corresponding author:** Ogundeji, O. O
Department of Mineral and Petroleum Engineering Technology, The Federal Polytechnic, Ado-Ekiti, Ekiti, State, Nigeria

Abstract

Grey cast iron (GCI) is characterized by brittleness, making it unsuitable for use in applications requiring high impact loading. Hence, efforts were made in this study to produce GCI with improved mechanical properties by addition of copper. Four samples were produced, the first sample was not alloyed (control), and the second, third and fourth were alloyed with 1.4wt.%Cu, 1.8wt.%Cu and 2.2wt.%Cu respectively. The samples were characterized using scanning electron microscope with EDS, and tested in tensile, hardness and impact. From the results, silicon contents of the alloyed samples are high relative to the control sample. The control and 2.2wt.%Cu alloyed samples are hypereutectic with carbon equivalent values (CEVs) of 4.391% and 4.200% respectively, while the 1.4wt.%Cu and 1.8wt.%Cu alloyed samples are hypoeutectic with CEVs of 3.940% and 3.600% respectively. The control sample is characterized by long graphite flakes, which are uniformly distributed within ferritic - pearlitic matrix. Graphite flakes of the 1.4 wt.% Cu and 1.8 wt.% Cu alloyed samples are uniformly distributed within pearlitic - ferritic matrix, while graphite flakes of the 2.2wt.%Cu alloyed sample are uniformly distributed within ferritic-pearlitic. Average graphite flake length of the control sample is high as compared to the copper alloyed samples, while graphite flake count of the control sample is low relative to the copper alloyed samples. Tensile strength characteristics of the copper alloyed samples are superior to the control sample. Optimum tensile strength characteristics (165.9 $Nm^{2)}$ was obtained at 1.4wt.%Cu. Ductile characteristic of the of control the sample is superior to ductile characteristics of the copper alloyed samples. Optimum ductility characteristic (3.82%) was obtained at 2.2 wt. %Cu. Hardness characteristics of the copper alloyed samples are superior to hardness characteristic of the control sample. Optimum hardness characteristics (61 HRB) was obtained at 1.4wt.%Cu. Impact strength characteristic of the control sample is low relative to impact strength characteristics of the copper alloyed samples. Optimum impact strength characteristics (78.93 $KJ/m^{2)}$ was obtained at 2.2wt.%Cu.

Keywords: Brittleness, impact loading, alloying, graphite flakes, pearlite-ferrite matrix; ferrite- pearlite matrix.

1. INTRODUCTION

Grey cast iron (GCI) is a family of cast iron with carbon content, ranging between 3-3.5%, and on the basis of matrix, grey cast iron can be classified as ferritic grey cast iron, pearlitic grey cast iron, ferritic - pearlitic grey cast iron and pearlitic – ferritic grey cast iron. In as-cast condition, microstructure of grey cast irons is often entirely pearlitic, with graphite lamellas finely distributed in the matrix (ASTM A247, 2006). Matrix structure of grey cast iron can be readily changed by heat treatment, while the flakes once formed, cannot be changed by heat treatment, however, quantity, shape and size of the graphite flakes may vary within a wide range (Pluphrach, 2010). GCI is characterized by good castability, wear resistance, machinability and high damping capacity, and according to Agunsoye *et al*., (2014) Fe-Cu alloy has shown to be a proven excellent material in vibration damping, particularly for shock absorbing applications, including engine blocks. GCI is used for brake components, electric-motors, pipes and machine bases (Seidu, 2014).

Mechanical properties of GCI are controlled by graphite flakes that are formed during solidification process, and mechanical behaviours are influenced by the amount of graphite and size, morphology and distribution of graphite lamellas (Das *et al.*, 2013; Collini *et al*., 2008; Hecht, 1999). Adedayo, (2013) revealed that microstructures of GCI was dependent significantly on heat storage capacity of the mold, and its mechanical properties were increased with increasing heat storage

capacity of the mold, Sahu *et al.*, (2014) attributed small and large graphite flake revealed by thin and large sections to fast and slow rates of cooling, Agunsoye *et al*., (2014) reported that impact energy of grey cast iron was improved with increasing percentage weight copper addition.

Past research findings have shown that tensile and shock resistance of GCI are less than steel (Collini *et al.*, 2008; Bates, 1997). Thus making steel a preferred choice material in application, requiring high strength and impact loading. This is in spite of low cost and ease of production of the former (Behnam *et al.*, 2010). No doubt, achieving improved mechanical properties in GCI requires proper casting practice. Consequently, in this study, efforts were at improving tensile and shock resistance of GCI through optimum copper addition requirements.

2. MATERIALS AND METHODS

2.1 Materials

The grey cast iron scrap used for this work was obtained from Oyerubulum Industrial Park, Akure, Ondo state. Nigeria. Other materials, which are copper wire, ferrosilicon, graphite and limestone were procured from the relevant vendors.

2.2 Methods

The charge (scrap and graphite) were broken down into smaller sizes to allow for easy passage through sprout of the rotary furnace. For effective melting and uniform melting rate, the rotary furnace was preheated for about 60-75 minutes before charging (Seidu, 2014). And further heated, the temperature was monitored and measured using optical pyrometer, and at 1485^{o}C, the charge had melted completely and ready for tapping into a ladle, which had been preheated to reduce temperature loss from molten metal. The melt was poured at temperature of 1450^{o}C into the wooden molds, containing rectangular metal patterns of dimensions 110 mm length, 12 mm breadth. The molds were prepared by mixing molding sand, bentonite, coal dust (additives) and water. And in order to allow for gradual transformation into a solid castings at room temperature, while ensuring avoidance of hot shaking effects on the solid state solidification, the molds were left for to 24hours (Sahu *et al.*, 2014).

During melt tapping, Fe-Si alloy inoculant (78% Si, 0.21% Al, Fe-bal.) of particle sizes ranged (0.5 - 1.5 mm) was added to the metal stream. The first melt, being the control sample was not alloyed, while the second, third and fourth melts were alloyed with 1.4wt.% Cu, 1.8wt.% Cu and 2.2wt.% Cu respectively. After the castings have completely solidified, they were knocked out of the molds, unwanted protrusions, including gating horns, fins and channel marks were cut off from the castings.

2.3 Microstructural examination

The control and copper alloyed samples were machined to standard metallographic samples in accordance with ASTM E3-11 (2011). Surfaces of the samples were flattened by cutting and filling and ground, using laboratory grinding machine with different sets of emery papers, starting from the coarsest to the finest. Orientation of the samples was changed during each round of ground. Emery papers of 60, 120, 240, 320, 400, 800 and 1200 grits were used. As the emery papers were changed from one to the other, the samples were turned through an angle of 90^{o} so as to remove scratches sustained from the previous grinding until a scratch-free surface was obtained. After which, they were polished, using laboratory polishing machine to give a mirror-like surface, using billiard cloth, washed with running water, cleaned with alcohol and dried in a warm air. And examined, using Philips SEM (XL30 TMP) scanning electron microscope (SEM) at x1000 magnification.

2.4 Mechanical testing

2.4.1 Hardness property

The castings were machined into hadness test specimens of dimensions 100 mm length and 10 mm breadth, grind and smoothened based on E384-11 (2011). Hardness measurementst were made, using Rockwell hardness tester, 60Kgf test force with indenter of known diameter was used. The indenter was pressed on the specimens surface with dwell time of 5 seconds. Indentation was made out at four different points, readings were taken and average values were taken and recorded. Fig 1 shows orthographic projections and isomeric diagram of the test specimen.

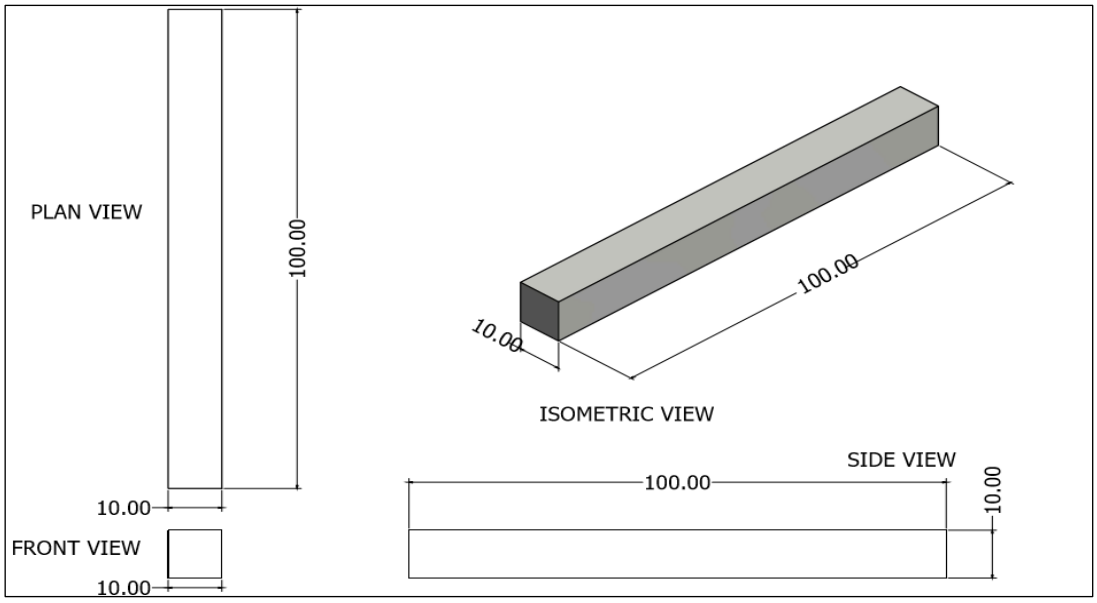

Fig 1: Hardness test specimen

2.4.2 Tensile property

Tensile test specimens were machined from the castings to 3.5 mm diameter (⌀) and 32 mm gauge length (L) in accordance with ASTM E 8-04 (2011), and placed in the proper grippers of INSTRON tensile testing machine, model 3369, and load was applied at the rate of 0.5mm/min. Orthographic projections and isomeric diagram of the test specimen are shown in Fig 2.

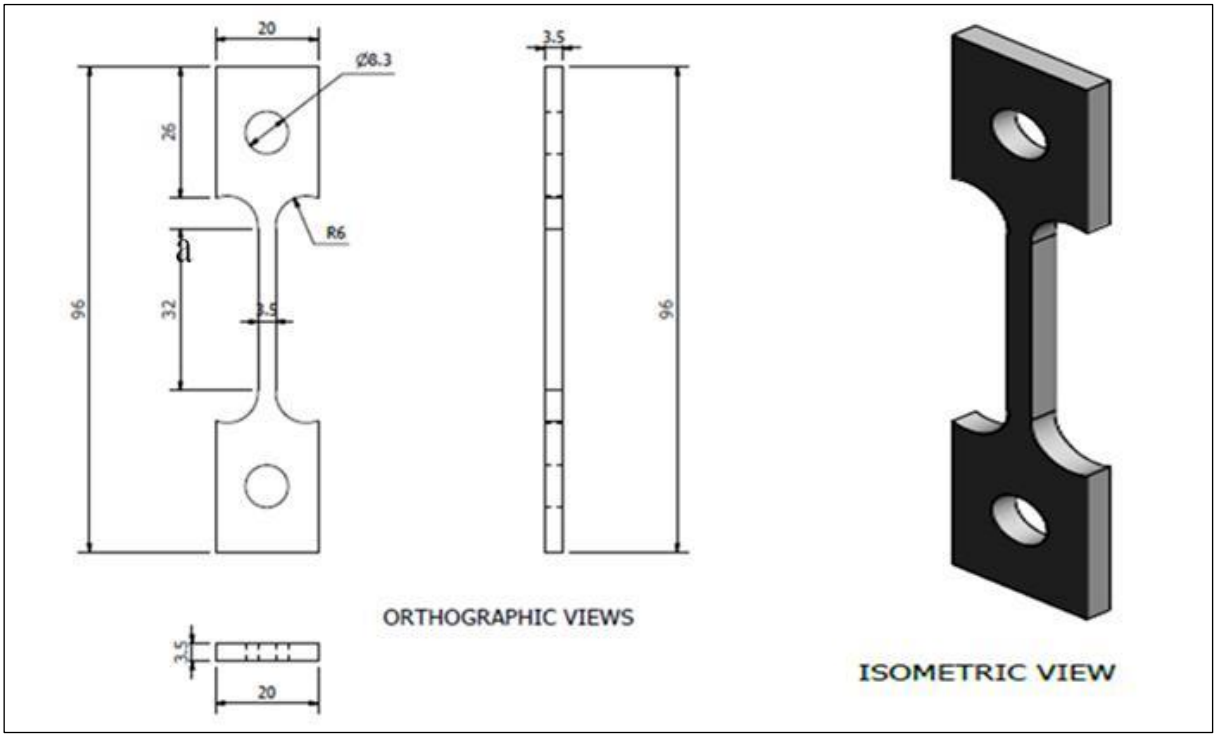

Fig 2: Tensile test specimen

2.4.3 Impact test

Impact test specimens with dimensions 100 mm length, 10 mm breadth and 8 mm deep V-notch at 45º were prepared in accordance with ASTM A370 (2011). The specimens were gripped horizontally, using vice, trigger of the INSTRON tensile testing machine (model 3369) was released, and energy absorbed in Joules to break the specimen registered by pointer of the quadrant scale was recorded. Fig 3 shows orthographic projections and isomeric diagram the impact test specimen.

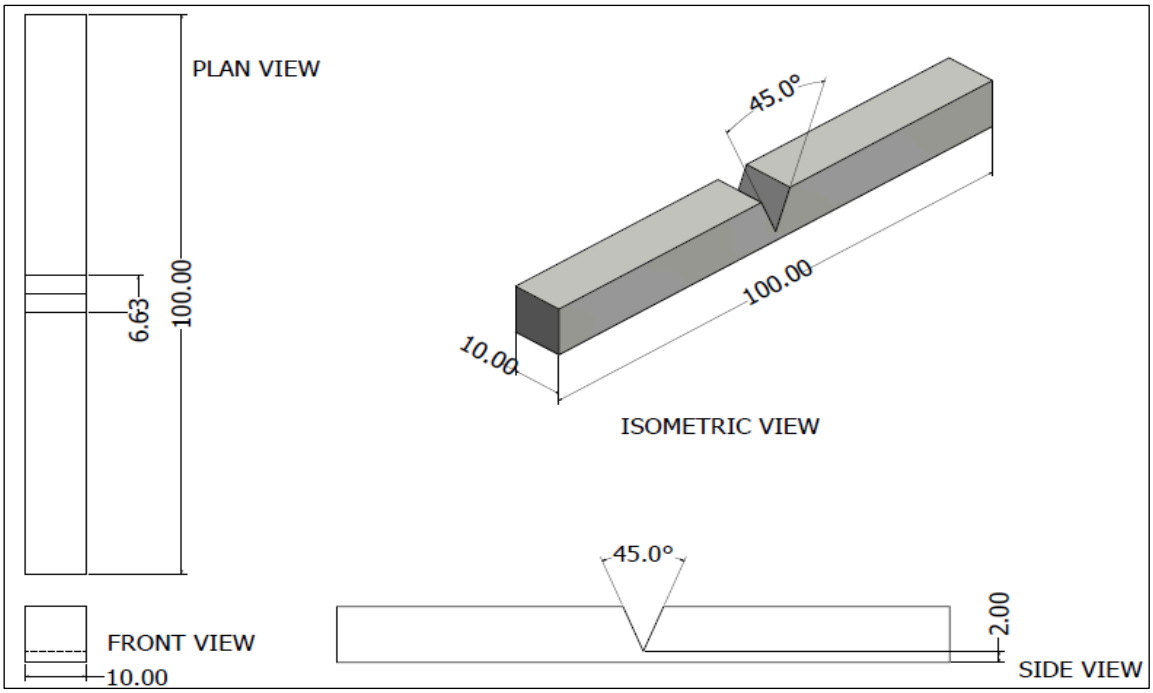

Fig 3: Impact test specimen

3. RESULTS AND DISCUSSION

3.1Chemical composition and carbon equivalent of the samples

From Table 1, High silicon contents of the alloyed samples relative to the control sample is suggestive high graphitization potential of the former. As a result, more volume fraction of pearlite may be revealed by the former than the later (Seidu, 2014; Agunsoye *et al.*, 2014). And from Table 3.2, the control and 2.2wt.%Cu alloyed samples with CEVs values of 4.391% and 4.200% respectively are hypereutectic GCI, while the 1.4wt.% and 1.8wt.% alloyed samples with the respective CEVs of 3.940% and 3.600% are hypoeutectic GCI. Hypereutectic and hypoeutectic GCI were due to fast and slow solidification rates respectively (Behnam *et al.*, 2010). At the fast cooling rate, formation of cementite (Fe_3C), which is characteristically a brittle phase may result (Johnson *et al.*, 2014; Khanna, 2002).

Table 1: Chemical compositions of the samples

Samples' descript.	C	Si	P	Cu	S	Ni	Mn	Al	Mo	Fe	CEV
Control	3.033	2.560	0.080	0.710	0.050	0.210	0.632	0.514	0.300	91.911	4.391
1.4%wt.Cu	2.900	3.075	0.045	1.630	<0.100	0.080	0.186	0.084	0.454	91.440	3.940
1.8%wt.Cu	2.650	2.800	0.040	1.918	<0.089	0.076	0.023	0.523	0.423	91.458	3.600
2.2%wt.Cu	3.327	2.629	0.004	1.843	0.002	0.043	0.018	0.080	0.037	92.019	4.200

3.2 MICROSTRUCTURE

3.2.1 Microstructures and EDS of the control and copper alloyed samples

Plate 1 is SEM micrograph of the control with EDS and SEM micrographs of the 1.4wt.%, 1.8wt.% and 2.2 wt.% copper alloyed samples are shown in Plates 2, 3 and 4 corresponding. The control sample is characterized by long graphite flakes, which are distributed uniformly within ferritic-pearlitic matrix, the 1.4 wt.% and 1.8 wt.% copper alloyed samples are comprised of shorter graphite flakes, which are distributed uniformly within pearlite-ferrite matrix, and the seemingly longer graphite flakes of the 2.2wt.% alloyed sample is distributed uniformly within ferritic-pearlitic matrix Sahu *et al*., 2014; Pluphrach, 2010).

From the EDS results, constituting elements of the control sample are Fe, C, O and Si, while those of 1.4wt.%Cu and 1.8 wt.% Cu are Mo, Mn, Fe and O C, Zn, Mg, Si and Mo, and are Cu, C,O, Na, Fe, Cu and Cl respectively. The constituting elements of 2.2wt.%Cu are O, Fe, Cu and Si. These elements occurred either in major or trace quantities. Graphite flake length (Fig.1) and graphite nodule count (Fig. 2), characterizing matrix of the GCI samples were due to relative graphitization effect of copper. Consequently, short graphite flake length and more graphite nodule count revealed by 1.4 wt.% Cu and 1.8 wt.% Cu alloyed samples resulted from high graphitization effect of copper, while long graphite flake and less graphite nodule count that characterized 2.2wt.%Cu was due to low graphitization effect of copper (Zou and Nakea, 2014; Tsuijikaiva, 2011).

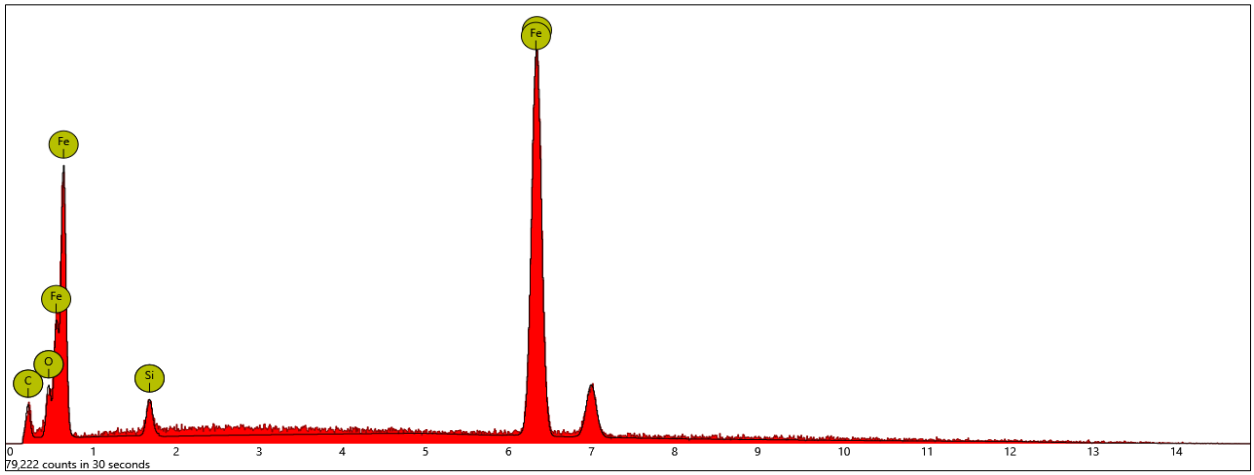

Plate 1: SEM of the control sample with EDS

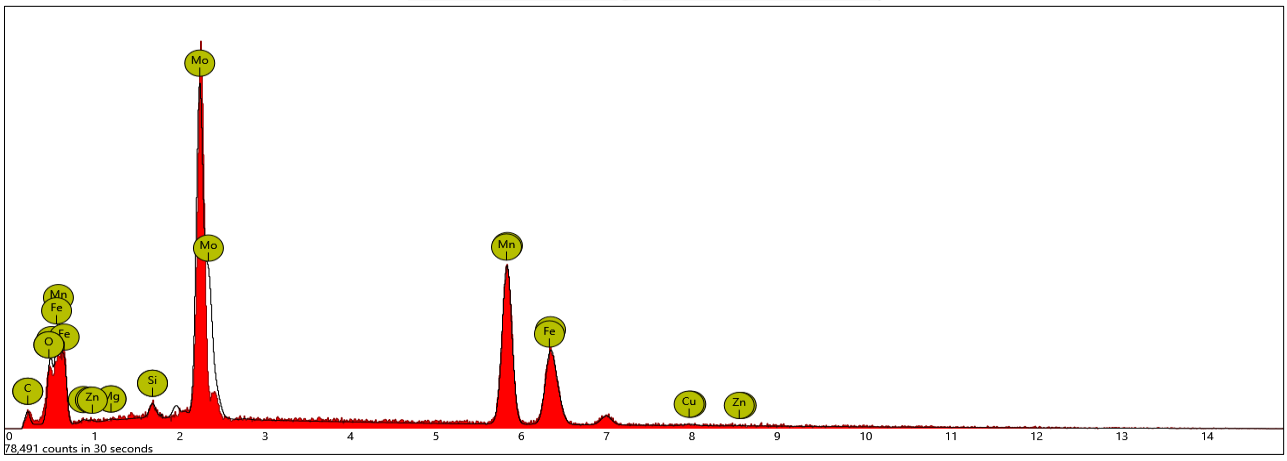

Plate 2: SEM of the 1.4 wt.% Cu alloyed sample with EDS

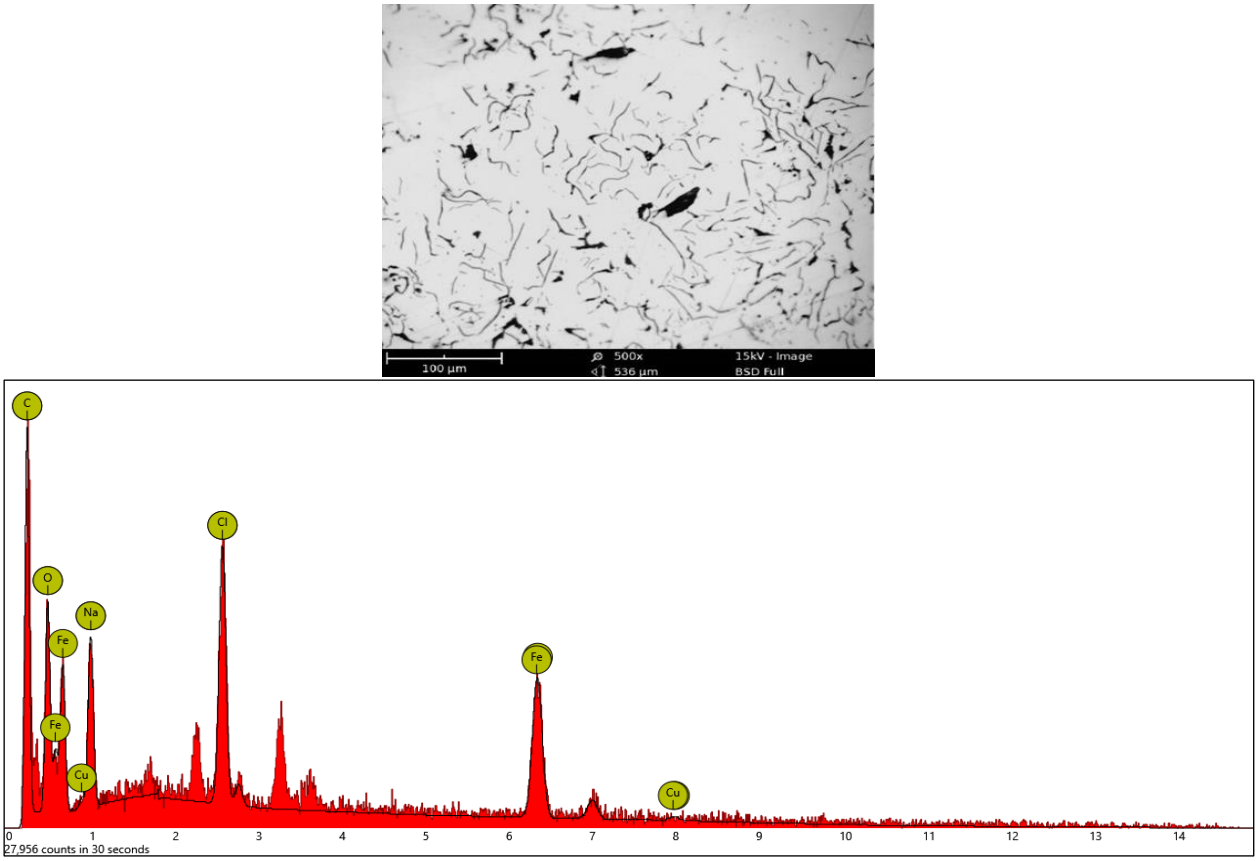

Plate 3: SEM of the 1.8 wt.% Cu alloyed sample with EDS

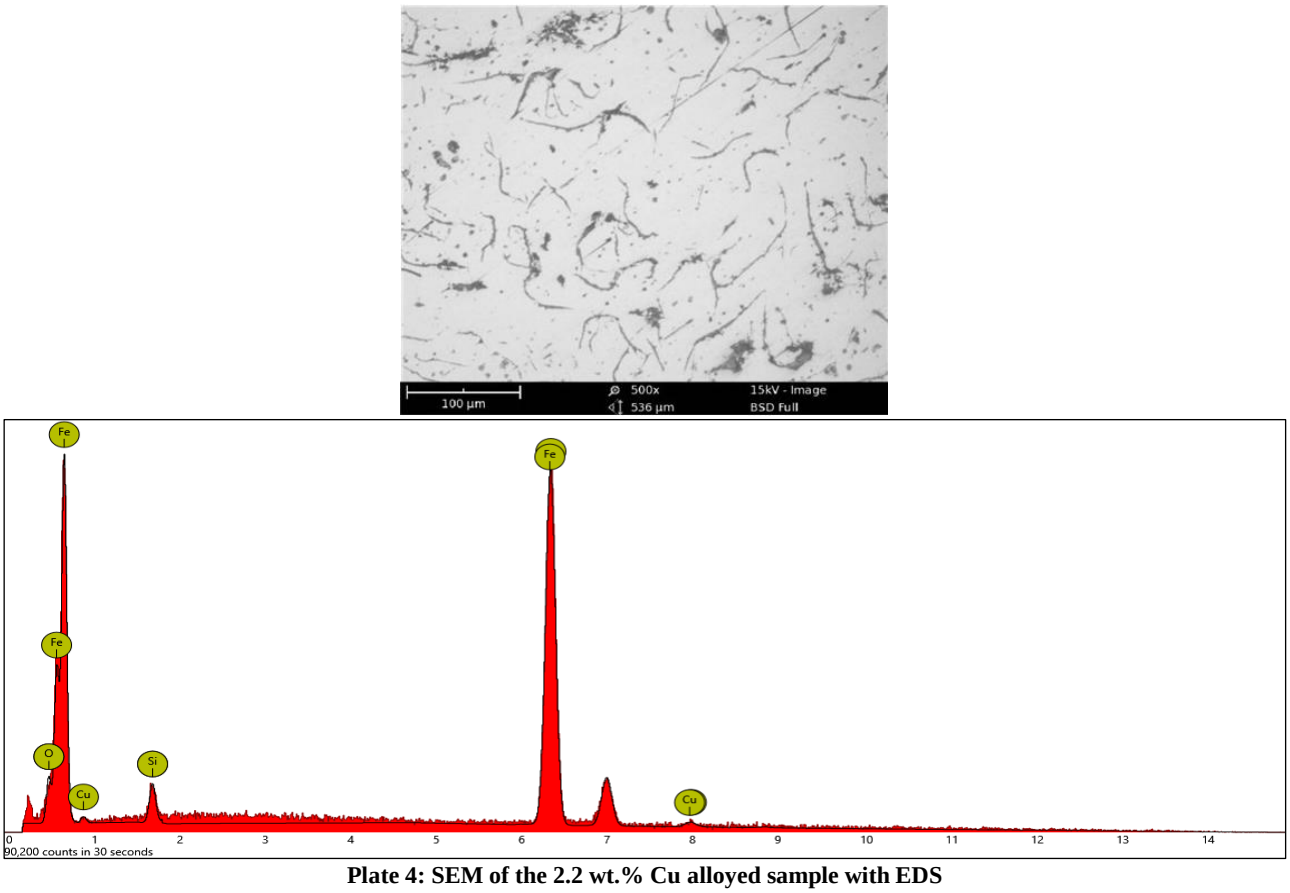

Plate 4: SEM of the 2.2 wt.% Cu alloyed sample with EDS

3.2.3 Average graphite flake length and graphite flake count

Figs 4 and 5 are the respective average flake length and graphite flake count of the grey cast iron samples. From the results, average flake length of the control sample is 130.50 µm, while average flake lengths of the 1.4wt.%Cu, 1.8wt.%Cu, and 2.2wt.%Cu alloyed samples are 100.77 µm, 104.46 and 109.78µm respectively. Graphite flake count of the control sample is 103, while graphite flake count of the 1.4wt.%Cu, 1.8wt.%Cu, and 2.2wt.%Cu alloyed samples are 179, 134 and 124 respectively.

In general, graphite flake length of the control sample is higher than those of the copper alloyed samples, while graphite flake count of the control sample is lower that of the copper alloyed samples. The increased in graphite flake length with concomitant decreased graphite flake count showed by the copper alloyed samples in the range of 1.4-1.8 wt. %Cu was due to increased more volume fraction of pearlite matrix of the GCI matrix, while the inverse at 2.2wt.% Cu resulted from more volume fraction of ferri in the matrix of the sample (Sahu *et al*. 2014; Tsuijikaiva, M. 2011; Hsu *et al*. 2000).

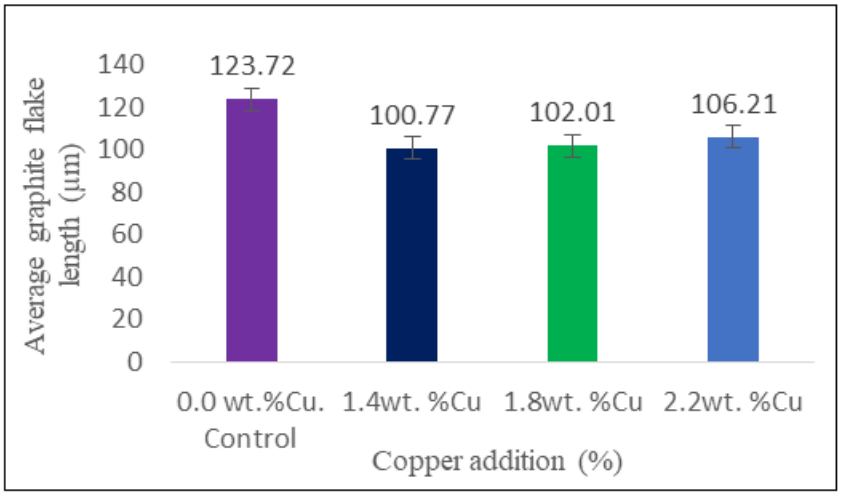

Fig 4: Influence of copper on the average graphite flake length of grey cast iron

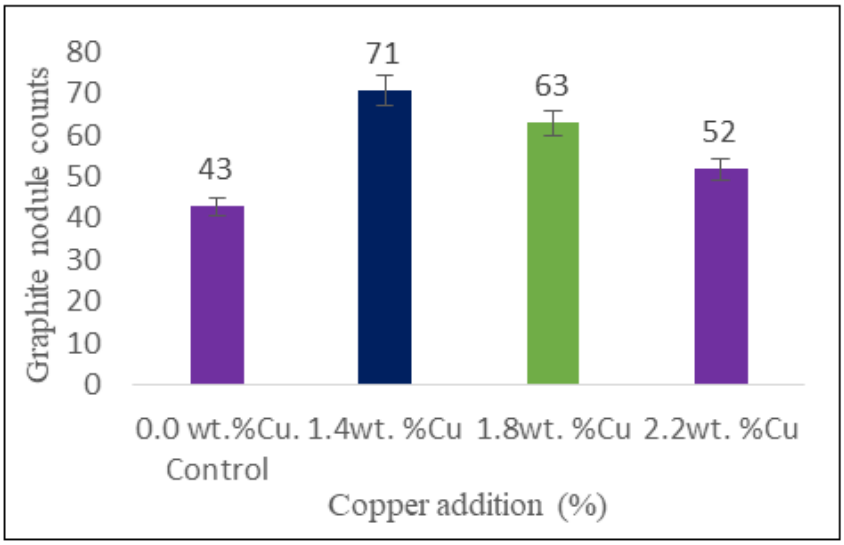

Fig 5: Influence of copper on the average graphite flake count of grey cast iron

3.3 MECHANICAL PROPERTIES

3.3.1 Tensile properties

Tensile strength characteristics of the control and copper alloyed samples are depicted in Fig 6 from the results, tensile strength value of the control sample is 136.25 N/mm^2 and tensile strength values of the 1.4wt.%Cu. 1.8wt.%Cu, and 2.2wt.%Cu alloyed samples are 165.9 Nm^2, 159.7 Nm^2 and 152.8 Nm^2 respectively. The superior tensile characteristics of copper alloyed samples over the control sample may be attributed to pearlite phase stabilization that resulted from graphitizing effect of copper (Collin *et al.*, 2008). In addition, short graphite flake length and more graphite nodule counts that resulted at 1.4wt.%Cu was contributory (Das *et al.*, 2013). Behnam *et al.*, (2010) have associated the presence of crack opening at the tip

and subsequent crack propagation through the microstructures of GCI to long flake length, explaining the inferior tensile behavior of 1.8wt.%Cu, and 2.2wt.%Cu alloyed samples, and hence optimum copper requirement for improved performance in tensile was achieved with 1.4wt.%Cu addition.

From Fig 7, percentage elongation value for the control is 3.61%, and those for the copper alloyed samples 1.4wt.%, 1.8wt.%, and 2.2wt.% copper alloyed are 3.47% and 3.82% respectively. Copper is a good graphitization, it promotes, refines and stabilizes pearlite and strengthen the matrix (Kovacs and Keough, 1993). Therefore, copper addition supports strength and hardness improvement at the expense of ductility. Therefore, it improves ductility at the expense, which explains the superior ductility of the control sample relative to the copper alloy samples. And the enhanced ductility behavior of the GCI in ascending order of 1.4wt.%, 1.8wt.% and 2.2 wt.% copper addition may be hinged on increasing presence of ferrite phase, Allan, (2012) have shown revealed that elongation property of DCI was enhanced by ferrite phase.

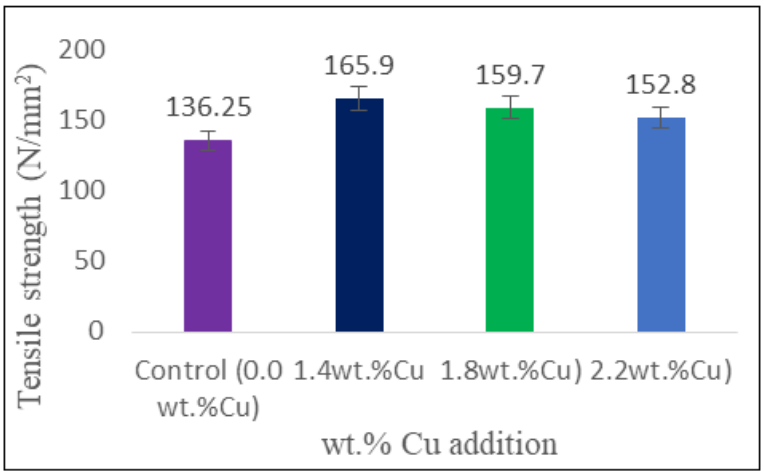

Fig 6: Influence of percent copper addition on tensile strength of the sample with 10 mm section thickness

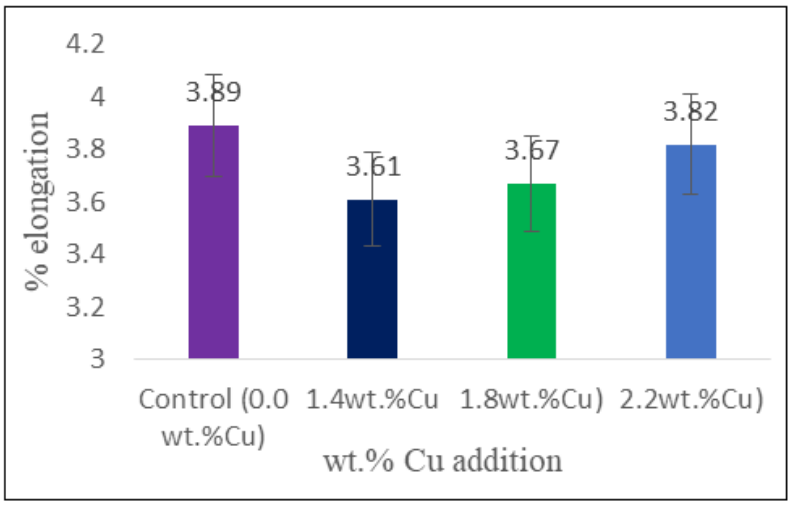

Fig 7: Influence of percent copper addition on % elongation of the samples with 10 mm section thickness

3.5.2 Hardness characteristic

Hardness characteristics of the control and copper alloyed samples are shown in Fig 8 From the results, hardness value of the control sample is 54 HRB, while hardness values of the 1.4wt.%, 1.8wt.%, and 2.2wt.% copper alloyed samples are 61 HRB, 59 HRB and 56 HRB respectively. The improved hardness characteristic of copper alloyed samples resulted from pearlite phase stabilization effect of copper (Hsu and Lin, 2011). The optimum hardness value at 1.4wt.% copper addition resulted from synergistic effect of pearlite stabilization and strengthening effect copper and the resulting shorter graphite flake length and more graphite nodule count in the GCI pearlitic-ferritic matrix (Tsuijikaiva, 2011). Cracks initiate more at tip of GCI with long graphite flakes (Hecht, 1999), therefore, decreasing hardness characteristic with increasing copper addition beyond 1.4wt.% at 1.8wt.% and 2.2wt.% was to be expected.

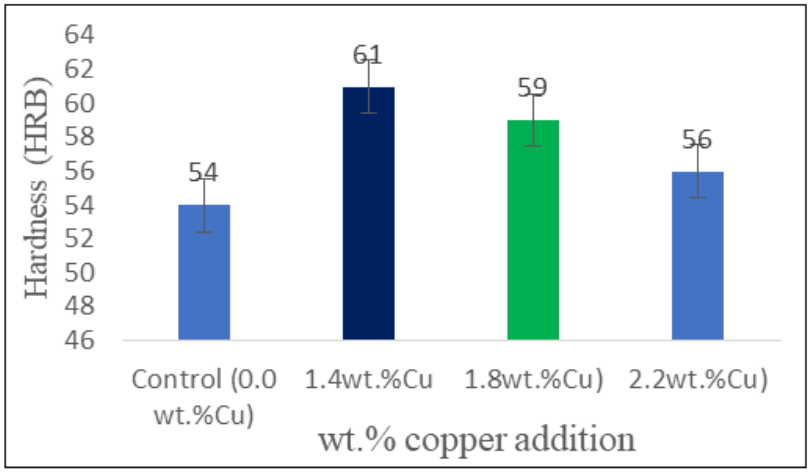

Fig 8: Influence of percent copper addition on hardness property of the samples with 10 mm section thickness

3.5.3 Impact strength

Fig 9 shows impact strength characteristics of the control and copper alloyed samples. From the results, impact strength value of the control sample is 71.66 KJ/m^2, while impact strength values of the 1.4wt.%, 1.8wt.%, and 2.2wt.% copper alloyed are 75.56 KJ/m^2, 72.37 KJ/m^2 and 78.93 KJ/m^2 respectively. Impact strength value of the control sample is low relative to the copper alloyed samples. In general, matrix with long and coarse graphite flakes are known to absorb more energy than matrix with fine and short flakes. Therefore, high (78.93 KJ/m^2) and low (72.37 KJ/m^2) impact strength values at 2.2wt.% and 1.8wt.% copper addition respectively are relatable to the resulting long and short graphite flakes length. Formation of ferritic- pearlitic matrix and the presence ledeburite, which is characteristically tough, ductile and soft contributed to optimum impact strength characteristic at 2.2wt.% copper addition (Hsu and Lin, 2011).

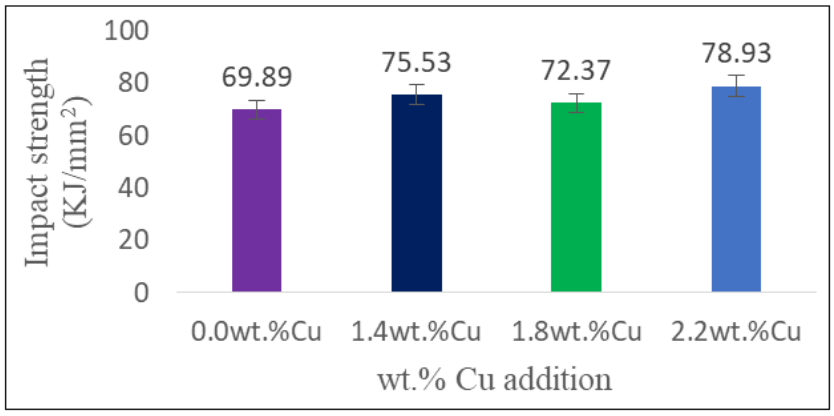

Fig 9: Influence varied percent copper addition on impact strength of the samples with 10 mm section thickness

4. CONCLUSIONS AND RECOMMENDATIONS

4.1 CONCLUSIONS

Based on the results obtained within the scope of this investigation, the following conclusions were drawn;

I. The control and 2.2wt.%Cu alloyed samples are hypereutectic with carbon equivalent values (CEV) of 4.391% and 4.200% respectively, while the 1.4wt.%Cu and 1.8wt.%Cu alloyed samples are hypoeutectic with CEVs of 3.940% and 3.600% respectively.

II. The control sample is characterized by long graphite flakes, which are uniformly distributed within ferritic-pearlitic matrix with the constituting elements Fe, C, O and Si.

III. Graphite flakes of the 1.4 wt.% Cu and 1.8 wt.% Cu alloyed samples are uniformly distributed within pearlite-ferrite matrix with the constituting elements: Mo, Mn, Fe, O, C, Zn, Mg, Si, Mo and C, O, Na, Fe, Cu respectively. Graphite flakes of the 2.2wt.%Cu alloyed sample are uniformly distributed within ferritic-pearlitic, and the constituting elements O, Fe, Cu and Si.

IV. Generally, average graphite flake length of the control sample is higher than those of the copper alloyed samples, while graphite flake count of the control sample is lower that of the copper alloyed samples.

V. Tensile strength characteristics of the copper alloyed samples are superior to the control sample, tensile strength value of the control sample is 136.25 N/mm^2 and tensile strength values of the 1.4wt.%Cu. 1.8wt.%Cu, and 2.2wt.%Cu alloyed samples are 165.9 Nm^2, 159.7 Nm^2 and 152.8 Nm^2 respectively. Optimum Tensile strength characteristics o was obtained at 1.4wt.%Cu.

VI. Ductile characteristic of the of control the sample is superior to ductile characteristics of the 1.4wt.%. 1.8wt.% copper alloyed samples and inferior to the 2.2wt.% copper alloyed sample. Percentage elongation value for the control is 3.61%, and percentage elongation values for the copper alloyed samples at 1.4wt.%Cu. 1.8wt.%Cu, and 2.2wt.%Cu are 3.47% and 3.82% respectively. Optimum ductility characteristics was obtained at 2.2 wt. %Cu.

VII. Hardness characteristics of the copper alloyed samples are superior to hardness characteristics of the control sample. Hardness value of the control sample is 54 HRB, while hardness values of the 1.4wt.%, 1.8wt.%, and 2.2wt.% copper alloyed samples are 61 HRB, 59 HRB and 56 HRB respectively. Optimum hardness characteristics was obtained at 1.4wt.%Cu.

VIII. Impact strength characteristic of the control sample is low relative to impact strength characteristics of the copper alloyed samples. Impact strength value of the control sample is 71.66 KJ/m^{2}and impact strength values of the 1.4wt.%, 1.8wt.%, and 2.2wt.% copper alloyed are 75.56 KJ/m^2, 72.37 KJ/m^2 and 78.93 KJ/m^2 respectively. Optimum impact strength characteristics was obtained at 2.2wt.%Cu.

REFERENCES

1. Adedayo, A.V. (2013). Relationship between graphite flake sizes and the mechanical properties of grey iron. *International Journal of Materials Science and Application, 2*(3), 94-98.
2. Agunsoye, J. O., Bello, S. A., Hassan, S. B., Adeyemo, R. G., & Odii, J. M. (2014), The effect of copper addition on the mechanical and wear properties of grey cast iron, *Journal of Minerals and Materials Characterization and Engineering*, 2, 470-483.
3. Allan, V. (2012). Microstructure and mechanical properties of austempered ductile iron, *Internal Journal of Engineering*, pp. 53-57.
4. American Standard for Testing and Measurement. (2007a). Standard test method and definitions for mechanical testing of steel products. *ASTM International*, 100 Barr Harbor Drive, West Conshohocken, PA 19428-2959 USA.
5. American Standard for Testing and Measurement A247. (2006). Standard test method for evaluating the microstructure of graphite in iron castings. *ASTM International*, 100 Barr Harbor Drive, West Conshohocken, pp19428-2959 USA.
6. American Standard for Testing and Measurement E3-11. (2011). Standard Guide for Preparation of Metallographic Specimens, ASTM International, West Conshohocken, www.astm.org
7. American Standard for Testing and Measurement E384-11. (2011). Standard Test Method for Microindentation Hardness of Materials, ASTM International. West Conshohocken, www.astm.org
8. American Standard for Testing and Measurement E8-04. (2008). Standard Test Methods for Tension Testing of Metallic Materials, ASTM International, West Conshohocken, www.astm.org
9. ASM Handbook. (2004). Metallography and Microstructures. Volume 9 pp 565-587. ASM International, Materials Park, Ohio, USA.
10. Bates, C. E. (1997). Effects of alloy elements on the strength and microstructure of grey cast iron",AFS Trans, pp. 923-946.
11. Behnam, M.M.J., Davami, P and Varahram, N. (2010). Effect of cooling rate on microstructure and mechanical properties of grey cast iron. *Materials Science and Engineering*, *A528*(2), 583–588.doi:10.1016/j.msea.2010.09.087
12. Collini, L., Nicoletto, G., & Konecna, R. (2008). Microstructure and mechanical properties of pearlitic grey cast iron. *Materials Science and Engineering*, A, *488*(1-2), 529–539.
13. Das, A. K., Dhal, J. P., Panda, R. K., Mishra S. C., & Sen, S. (2013). Effect of alloying elements and processing parameters on mechanical properties of austempered ductile iron. *Journal of Materials and Metallurgical Engineering, 3*(1), pp. 8-16.
14. Hecht, R. L. (1999). The effect of graphite flakes morphology on the thermal diffusivity of cast irons, *Journal of Material Science*, 34, 4775-4781.
15. Hsu, C. H., & Lin, K. T. (2011). A study on microstructure and toughness of copper alloyed and austemperedductile irons. *Materials science and engineering* A, 528, pp.5706-5712.
16. Johnson, O. A., Sefiu, A. B., Bolaji, H., & Adeyemo, R. G. (2014). The Effect of copper addition on the mechanical and wear properties of grey cast iron, *Journal of Minerals and Materials Characterization and Engineering*, *2*(5), 470-483.
17. Khanna, O. P. (2002). *A textbook of Foundry Technology* (9th ed., pp.431).
18. Kovacs B. V., & Keough, J. R. (1993). Physical properties and application of austempered gray iron, *AFS Transaction*, 101, pp. 283-291.
19. Pluphrach, G. (2010). Study of the effect of solidification on graphite flakes microstructure and mechanical properties of an ASTM a-48 grey cast iron using steel molds. *Songklanakarin Journal of Science and Technology*, *32*(6), 613-618.
20. Sahu, S., Bhat, M. N., Kumar, A., Pratik, A., & Kumar, A. (2014). Effect of section thickness on the microstructure and hardness of grey cast iron(A

Simulation Study).*International Journal of Engineering Research &Technology*, *3*(7), 35- 40.
21. Seidu, S. O. (2014). Effect of compositional changes on the mechanical behavior of grey cast iron, *Journal of Metallurgical Engineering*, *3*(2).
22. Tsuijikaiva, M. (2011). Pearlite stabilization by copper on ductile cast iron. *Key Engineering Materials and Technology*, 457, 151-156.
23. Zou, Y., & Nakea, H. (2014). Influence of boron on ferrite formation in copper added spheroidal graphite cast iron. *Journal of China Foundry*, *11*(4), 375-381.